

HEAD2TOE: UTILIZING INTERMEDIATE REPRESENTATIONS FOR BETTER TRANSFER LEARNING

Utku Evci, Vincent Dumoulin, Hugo Larochelle, Michael C. Mozer

Google Research, Brain Team

{evcu, vdumoulin, hugolarochelle, mcmozer}@google.com

ABSTRACT

Transfer-learning methods aim to improve performance in a data-scarce target domain using a model pretrained on a data-rich source domain. A cost-efficient strategy, *linear probing*, involves freezing the source model and training a new classification head for the target domain. This strategy is outperformed by a more costly but state-of-the-art method—*fine-tuning* all parameters of the source model to the target domain—possibly because fine-tuning allows the model to leverage useful information from intermediate layers which is otherwise discarded by the later pretrained layers. We explore the hypothesis that these intermediate layers might be directly exploited. We propose a method, *Head-to-Toe probing* (HEAD2TOE), that selects features from all layers of the source model to train a classification head for the target-domain. In evaluations on the Visual Task Adaptation Benchmark (VTAB), Head2Toe matches performance obtained with fine-tuning on average while reducing training and storage cost hundred folds or more, but critically, for out-of-distribution transfer, Head2Toe outperforms fine-tuning.¹

1 INTRODUCTION

Transfer learning is a widely used method for obtaining strong performance in a variety of tasks where training data is scarce; see Zhu et al. (2020), Alyafeai et al. (2020), and Zhuang et al. (2020) for recent application-specific surveys. A well-known recipe for transfer learning involves the supervised or unsupervised pretraining of a model on a *source* task with a large training dataset (also referred to as *upstream training*). After pretraining, the model’s output head is discarded, and the rest of the network is used to obtain a feature embedding, i.e., the output of what was formerly the penultimate layer of the network. When transferring to a *target* task, a new output head is trained on top of the feature extractor (*downstream training*). This approach makes intuitive sense: if a linear combination of embedding features performs well on the source task, we expect a different linear combination of features to generalize to the target domain, provided the source and target domains are similar.

This approach of training a new output head, referred to as *linear probing* (LINEAR), often yields significant improvements in performance on the target task over training the network from scratch (Kornblith et al., 2019). An alternative to LINEAR is *fine-tuning* (FINETUNING), which uses target-domain data to adapt all weights in the feature extractor together with the new output head. This procedure requires doing forward and backward passes through the entire network at each training step and therefore its per-step cost is significantly higher than LINEAR. Furthermore, since the entire network is fine-tuned, the entire set of new weights needs to be stored for every target task, making FINETUNING impractical when working on edge devices or with a large number of target tasks. However, FINETUNING is often preferred over LINEAR since it consistently leads to better performance on a variety of target tasks even when data is scarce (Zhai et al., 2019).

FINETUNING’s superior generalization in the low-data regime is counterintuitive given that the number of model parameters to be adapted is often large relative to the amount of available training data. How does FINETUNING learn from few examples successfully? We conjecture that FINETUNING better leverages existing internal representations rather than discovering entirely new representations; FINETUNING exposes existing features buried deep in the net for use by the classifier. Under

¹We open source our code at <https://github.com/google-research/head2toe>.

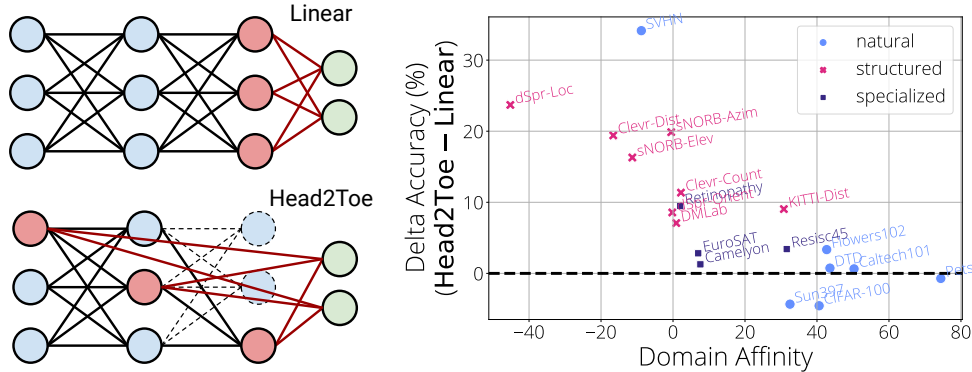


Figure 1: **(left)** Whereas LINEAR utilizes only the last layer for transfer to a new output head (green), HEAD2TOE selects the most useful features from the entire network and trains a linear head on top. **(right)** HEAD2TOE obtains better transfer accuracy than LINEAR; especially for OOD domains (left side of the plot). Domain affinity (defined in Section 2) is used to sort domains on the x-axis and aims to capture how similar a target domain is compared to the source dataset (ImageNet in this case).

this hypothesis, *features needed for transfer are already present in the pretrained network and might be identified directly without fine-tuning the backbone itself*. In Section 3.1, we argue that FINETUNING can be approximated by a linear probe operating on features from lower layers of the net, thus enabling state of art transfer performance with significantly less cost.

In this work, we propose and explore methods for selecting useful features from *all* layers of a pretrained net, including the embedding, and then applying the LINEAR transfer approach to the constructed representation. Compare the standard approach in the upper diagram of Fig. 1-left to our approach, called head-to-toe probing (HEAD2TOE), in the lower diagram. Our approach leads to significant improvements over LINEAR (Fig. 1-right) and matches FINETUNING performance on average. Our key contributions are as follows:

1. We observe a strong correlation between the degree to which a target domain is out-of-distribution (OOD) with respect to the source domain and the benefit of incorporating intermediate representations in LINEAR (Fig. 1-right and Section 3.3).
2. We introduce HEAD2TOE, an efficient transfer learning method for selecting relevant features from intermediate representations (Section 3.3).
3. On the VTAB collection of data sets, we show that HEAD2TOE outperforms LINEAR and matches the performance of more computationally costly FINETUNING with only 0.6% of the training FLOPs and 1% of the storage cost (Section 4).
4. Critically, HEAD2TOE outperforms FINETUNING on OOD target domains. If a practitioner can make an educated guess about whether a target domain is OOD with respect to a source, using HEAD2TOE improves on the state of the art for transfer learning.

2 PRELIMINARIES

Source domain and backbone models. In our experiments, we use source models pretrained on ImageNet-2012 (Russakovsky et al., 2015), a large scale image classification benchmark with 1000 classes and over million natural images. We benchmark HEAD2TOE using convolutional (ResNet-50, Wu et al., 2018) and attention-based (ViT-B/16, Dosovitskiy et al., 2021) architectures pretrained on ImageNet-2012.

Target domains. In this work, we focus on target tasks with few examples (i.e., *few-shot*) and use Visual Task Adaptation Benchmark-1k (Zhai et al., 2019) to evaluate different methods. Visual Task Adaptation Benchmark-1k consists of 19 different classification tasks, each having between 2 to 397 classes and a total of 1000 training examples. The domains are grouped into three pri-

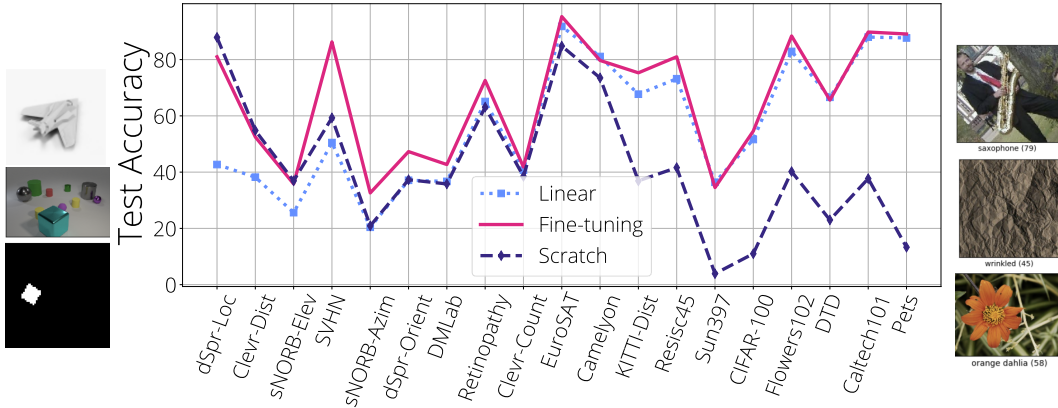


Figure 2: **Characterizing out-of-distribution (far) domains** Generalization performance of various baselines on the VTAB-1k benchmark using ResNet-50 architecture and 224 image size. The architecture is pretrained on ImageNet-2012 for the transfer learning (TL) baselines. Datasets (and the three groups of the benchmark) are ordered according to their Domain Affinity scores in ascending order from left to right. Examples from the left- and right-most datasets are also shown on corresponding sides.

many categories: (1) natural images (*natural*), (2) specialized images using non-standard cameras (*specialized*), and (3) rendered artificial images (*structured*).

Characterizing out-of-distribution (far) domains. Consider the relationship between source and target domains. If the domain overlap is high, then features extracted for linear classification in the source domain should also be relevant for linear classification in the target domain, and LINEAR should yield performance benefits. If the domain overlap is low, then constraining the target domain to use the source domain embedding may be harmful relative to training a model from scratch on the target domain. Therefore, we might quantify the source-target distribution shift in terms of how beneficial LINEAR is relative to training a model from scratch (denoted SCRATCH):

$$\text{DomainAffinity} = \text{Acc}_{\text{LINEAR}} - \text{Acc}_{\text{SCRATCH}}.$$

In Fig. 2 (also Fig. 1-right), the 19 VTAB-1k target tasks are arranged from low to high by their domain affinity to ImageNet-2012 for a pretrained ResNet-50 backbone. The left and right ends of Fig. 2 show examples of the three target domains with the most and least distribution shift, respectively. These examples seem consistent with intuitive notions of distribution shift.

Baselines. Fig. 2 also presents transfer test accuracy of LINEAR, FINETUNING, and SCRATCH baselines. Consistent with the literature, FINETUNING performs as well or better than the other two baselines. For in-distribution targets (right side of graph), LINEAR matches FINETUNING; for OOD targets (left side of graph), LINEAR is worse than FINETUNING. With distribution mismatch, the source network may filter information available in lower layers because it is not needed for the source task but is essential for the target task. Observing FINETUNING performs better than SCRATCH even in OOD tasks, we hypothesize that intermediate features are key for the FINETUNING, since if learning novel features was possible using limited data, training the network from scratch would work on-par with FINETUNING. Motivated by this observation, HEAD2TOE probes the intermediate features of a network directly and aims to match the fine-tuning results without modifying the backbone itself.

3 HEAD2TOE UTILIZATION OF PRETRAINED BACKBONES

3.1 TAYLOR APPROXIMATION OF FINE-TUNING

Maddox et al. (2021) and Mu et al. (2020) observe that the parameters of a pre-trained backbone change very little during fine-tuning and that a linearized approximation of the fine-tuned model can be used to obtain competitive results in transfer learning. Here we follow a similar motivation and

argue that the linearized fine-tuning solution should be well captured by a linear combination of the intermediate activations.

To demonstrate our intuition, consider a multi-layer, fully-connected neural network with a scalar output $F(x; w)$ parameterized by weights w where x is the input. Let’s denote the individual elements of w by w_{ij} , where the indices reflect the neurons connected such that the activations of neurons are given by $z_j = \sum_i w_{ij} h_i$ and $h_i = f(z_i)$ where f is the activation function used in the network. Then, we can write the fine-tuned neural network (parameterized by optimized parameters w^*) using the first-order Taylor approximation:

$$F(x; w^*) \approx F(x; w) + \sum_{i,j} \frac{\partial F(x; w)}{\partial w_{ij}} \Delta w_{ij}$$

where $\Delta w_{ij} = w_{ij}^* - w_{ij}$ reflects the displacement of updated weights during fine-tuning. Expanding the gradient term using the chain rule and rearranging the summations, the linearized solution found by FINETUNING can be written as a linear combination of the intermediate activations:

$$\begin{aligned} F(x; w^*) &\approx F(x; w) + \sum_{i,j} h_i \frac{\partial F(x; w)}{\partial z_j} \Delta w_{ij} \\ &\approx F(x; w) + \sum_i h_i \sum_j \frac{\partial F(x; w)}{\partial z_j} \Delta w_{ij} \\ &\approx F(x; w) + \sum_i h_i c_{i,x} \end{aligned}$$

Thus, for a given input x , the FINETUNING solution can be approximated by a linear combination of activations of all features in the network, where the coefficients, $c_{i,x}$, are obtained using the same method as LINEAR. This approximate equivalence holds so long as fine-tuning produces small displacements Δw_{ij} , which supports our hypothesis that using intermediate activations can help bridge the gap between FINETUNING and LINEAR.

3.2 YOUR REPRESENTATIONS ARE RICHER THAN YOU THINK

In this section, we conduct a simple experiment to demonstrate the potential of using representations from intermediate layers. We concatenate the feature embedding of a pretrained ResNet-50 backbone (features from the penultimate layer) with features from *one* additional layer and train a linear head on top of the concatenated features. When extracting features from convolutional layers, we reduce the dimensionality of the convolutional stack of feature maps using strided average pooling, with a window size chosen so that the resulting number of features is similar to the number of embedding features (2048 for ResNet-50).

To estimate an upper bound on performance improvement over LINEAR by including a single intermediate layer, we use an oracle to select the layer which yields the largest boost in test performance (separately for each target task). Percentage improvement over LINEAR using this ORACLE is shown in Fig. 3-left. We observe a Spearman correlation of -0.75 between the domain affinity of a target task and the accuracy gain. In accordance with our hypothesis, adding intermediate representations does not improve in-domain generalization because the feature embedding already contains the most useful features. In contrast, generalization on out-of-domain tasks are improved significantly when intermediate features are used.

In Fig. 3-top-right, we show test accuracy for two domains as a function of the ResNet-50 layer whose internal representation is used to augment the feature embeddings. Figures for the remaining tasks can be found in Appendix D. Different tasks on the VTAB benchmark benefit from the inclusion of different layers to obtain the best generalization accuracy, which emphasizes the importance of domain-specific selection of the right set of features for optimal generalization. Overall, the ORACLE that selects the layer with best test performance for each task yields an average of 3.5% improvement on VTAB-1k benchmark. One possible explanation for the improvement in performance with the augmented representation is simply that it has more degrees of freedom (4096 features instead of 2048). To demonstrate that the improvement is due to inclusion of intermediate layers and not simply due to increased dimensionality, Fig. 3-bottom-right compares the ORACLE to

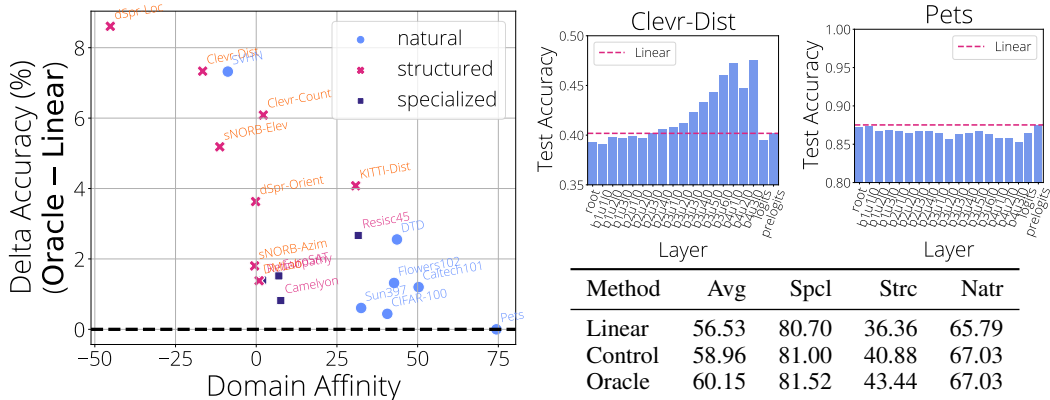


Figure 3: **(left)** Accuracy gains when prelogits are augmented with an additional layer correlates negatively (-0.745 , Spearman) with domain affinity. **(right-top)** effect of using features from intermediate layers for Clevr-Dist (low domain affinity) and Pets (high domain affinity) tasks **(right-bottom)** Test accuracies of various baselines on VTAB-1k. *Linear* uses only prelogits, *Oracle* averages are obtained by using the layer that gives best generalization (test) for each task. *Control* experiment uses a second feature embedding from a second pretrained network trained using a different seed. We use ResNet-50 models pretrained on ImageNet-2012.

a CONTROL condition whose representation is matched in dimensionality but formed by concatenating a feature embedding obtained from a second ResNet-50 backbone pretrained on ImageNet-2012. Note that this experiment bears similarity to *ensembling* (Zhou et al., 2002), which is known to bring significant accuracy gains on its own (Mustafa et al., 2020). Utilizing a second backbone doubles the amount of resources required, yet it falls 1% shy of ORACLE performance, demonstrating the extent to which using intermediate representations can be helpful for generalization.

3.3 HEAD2TOE

Motivated by our observations in the previous section, we hypothesize that we can attain—or possibly surpass—the performance of FINETUNING without modifying the backbone itself by using LINEAR augmented with well-chosen intermediate activations. Our investigation leads us to HEAD2TOE, an efficient transfer learning algorithm based on utilizing intermediate activations using feature selection.

Notation. Our method applies to any network with any type of layers, but here, for simplicity and without loss of generality, we consider a network with L fully connected layers, each layer receiving input from the layer below:

$$\mathbf{z}_\ell = \mathbf{h}_{\ell-1} \mathbf{W}_\ell \quad ; \quad \mathbf{h}_\ell = f(\mathbf{z}_\ell) \quad (1)$$

where the subscript denotes a layer index, $\mathbf{h}_0 = \mathbf{x}$ is the input, f is the activation function, \mathbf{W}_ℓ is the weight matrix of layer ℓ , and \mathbf{z}_L is the logit vector used for classification. When transferring a pretrained network to a target task using LINEAR, we discard the last layer of the pretrained network and train a new set of linear weights, \mathbf{W}'_L , such that predictions (logits) for the new task are obtained by $\mathbf{z}'_L = \mathbf{h}_{L-1} \mathbf{W}'_L$.

Head2Toe. Consider a simple scheme that augments the backbone embedding with activations from all layers of the network, such that:

$$\mathbf{z}'_L = \mathbf{h}_{all} \mathbf{W}_{all} \quad ; \quad \mathbf{h}_{all} = \text{concat}(a_1(\mathbf{h}_1), a_2(\mathbf{h}_2), \dots, a_L(\mathbf{h}_L)) \quad (2)$$

where $a_\ell(\cdot)$ denotes a fixed function to reduce the dimensionality of the activation vector and normalize at a given layer ℓ . Such functions become valuable when considering network architectures like convolutional networks that generate large number of intermediate features. Though better aggregation schemes may exist, we simply perform one or two-dimensional strided average pooling to reduce dimensionality. After aggregation, we normalize features coming from each layer to a unit

norm. This scaling preserves the relative magnitude of features within a layer while accounting for inter-layer differences and works better than normalizing each feature separately or not normalizing at all.

Even with dimensionality reduction, \mathbf{h}_{all} can exceed a million elements, and \mathbf{W}_{all} is underconstrained by the training data, leading to overfitting. Further, \mathbf{W}_{all} may become so large as to be impractical for deploying this model.² We can address these issues by selecting a subset of features before training the target-domain classifier.

Feature selection based on group lasso. Group lasso (Yuan & Lin, 2006) is a popular method for selecting relevant features in multi-task adaptation settings (Argyriou et al., 2007; Nie et al., 2010). When used as a regularizer on a weight matrix \mathbf{W} , the group-lasso regularizer encourages the ℓ_2 norm of the rows of the matrix to be sparse, and is defined as:

$$|\mathbf{W}|_{2,1} = |\mathbf{s}|_1 = \sum_i |s_i|, \quad \text{where} \quad s_i = \sqrt{\sum_j w_{ij}^2}. \quad (3)$$

To determine which features are most useful for the task, the linear head is trained with group-lasso regularization on \mathbf{W}_{all} . In contrast to the approach taken by Argyriou et al. (2007) and Nie et al. (2010), which use costly matrix inversions, we incorporate the regularization as a secondary loss and train with stochastic gradient descent. Following training, *relevance scores* for each feature i , s_i , are computed. We select a fraction F of the features with largest relevance and train a new linear head to obtain the final logit mapping. Feature selection alone provides strong regularization, therefore during the final training we do not use any additional regularization.

We make two remarks here. First, because the initial round of training \mathbf{W}_{all} with the group-lasso regularizer is used only to rank features by importance, the method is quite robust to the regularization coefficient; it simply needs to be large enough to distinguish the contribution of the individual features. Second, interpreting s_i as the importance of feature i depends on all features having the same dynamic range. This constraint will often be satisfied naturally due to the normalization done after aggregation as explained previously.

Selection of F . The fraction F determines the total number of features retained. One would expect the optimal value to depend on the target task. Therefore, we select F for each task separately by cross-validation on the training set. This validation procedure is inexpensive compared to the cost of the initial phase of the algorithm (i.e., training of \mathbf{W}_{all} to obtain \mathbf{s}) due to the reduced number of features in the second step. Overall, HEAD2TOE together with its validation procedure requires 18% more operations compared to training \mathbf{W}_{all} alone (details shared in Appendix B).

Cost of HEAD2TOE. HEAD2TOE’s use of a fixed backbone means that as we search for features to include, the actual features values are fixed. Consequently, we can calculate them once and re-use as necessary, instead of recalculating at every step, as required for FINETUNING. Furthermore, since the backbone is frozen, the storage required for each target task includes only the final output head and the binary mask indicating the features selected. Due to these properties, the cost of HEAD2TOE follows the cost of LINEAR closely while being significantly less than FINETUNING. A detailed cost analysis can be found in Appendix B.

4 EVALUATING HEAD2TOE

We evaluate HEAD2TOE on the VTAB-1k benchmark using two popular vision architectures, ResNet-50 (Wu et al., 2018) and ViT-B/16 (Dosovitskiy et al., 2021), both pretrained on ImageNet-2012. ResNet-50 consists of 50 convolutional layers. To utilize the intermediate convolutional features, we aggregate spatial information using average pooling on non-overlapping patches, as explained in Section 3.3. We adjust the pooling size to target a fixed dimensionality of the representation. For example, for a feature map of shape $20 \times 20 \times 128$ and a *target size* of 512, we average-pool disjoint patches of size 5×5 , resulting in 4 features per channel and 1024 features in total. This helps us to balance different layers in terms of the number features they contribute to the

²For example, using a pooling size of 2, ResNet-50 generates 1.7 million features and storing \mathbf{W}_{all} requires 6.6e8 parameters (2.6GB for float32) for SUN-397.

	Natural							Specialized				Structured							Mean	
	CIFAR-100	Caltech101	DTD	Flowers102	Pets	SVHN	Sun397	Camelyon	EuroSAT	Resisc45	Retinopathy	Clevr-Count	Clevr-Dist	DMLab	KITTI-Dist	dSpr-Loc	dSpr-Ori	sNORB-Azim		sNORB-Elev
Linear	48.5	86.0	67.8	84.8	87.4	47.5	34.4	83.2	92.4	73.3	73.6	39.7	39.9	36.0	66.4	40.4	37.0	19.6	25.5	57.0
+All- ℓ_2	44.7	87.0	67.8	84.2	86.1	81.1	31.9	82.6	95.0	76.5	74.5	50.0	56.3	38.3	65.5	59.7	44.5	37.5	40.0	63.3
+All- ℓ_1	50.8	88.6	67.4	84.2	87.7	84.2	34.6	80.9	94.9	75.6	74.7	49.9	57.0	41.8	72.9	59.0	44.8	37.5	40.8	64.6
+All- $\ell_{2,1}$	49.1	86.7	68.5	84.2	88.0	84.4	34.8	81.5	94.9	75.7	74.3	48.3	58.4	42.0	74.4	58.8	45.2	37.8	34.4	64.3
Head2Toe	47.1	88.8	67.6	85.6	87.6	84.1	32.9	82.1	94.3	76.0	74.1	55.3	59.5	43.9	72.3	64.9	51.1	39.6	43.1	65.8
Fine-tuning*	54.6	89.8	65.6	88.4	89.1	86.3	34.5	79.7	95.3	81.0	72.6	41.8	52.5	42.7	75.3	81.0	47.3	32.6	35.8	65.6
Scratch*	11.0	37.7	23.0	40.2	13.3	59.3	3.9	73.5	84.8	41.6	63.1	38.5	54.8	35.8	36.9	87.9	37.3	20.9	36.9	42.1

	Natural							Specialized				Structured							Mean	
	CIFAR-100	Caltech101	DTD	Flowers102	Pets	SVHN	Sun397	Camelyon	EuroSAT	Resisc45	Retinopathy	Clevr-Count	Clevr-Dist	DMLab	KITTI-Dist	dSpr-Loc	dSpr-Ori	sNORB-Azim		sNORB-Elev
Linear	55.0	81.0	53.6	72.1	85.3	38.7	32.3	80.1	90.8	67.2	74.0	38.5	36.2	33.5	55.7	34.0	31.3	18.2	26.3	52.8
+All- ℓ_2	57.3	87.0	64.3	82.8	84.0	75.7	32.4	82.0	94.7	79.7	74.8	47.4	57.8	41.4	62.8	46.6	33.3	31.0	38.8	61.8
+All- ℓ_1	58.4	87.3	64.9	83.3	84.6	80.0	34.4	82.3	95.6	79.6	73.6	47.9	57.7	42.2	65.1	44.5	33.4	32.4	38.4	62.4
+All (Group)	59.6	87.1	64.9	85.2	85.4	79.5	35.3	82.0	95.3	80.6	74.2	47.9	57.8	40.7	64.9	46.7	33.6	31.9	39.0	62.7
Head2Toe	58.2	87.3	64.5	85.9	85.4	82.9	35.1	81.2	95.0	79.9	74.1	49.3	58.4	41.6	64.4	53.3	32.9	33.5	39.4	63.3
Fine-tuning	45.0	84.3	53.8	85.4	75.4	84.0	26.7	85.4	95.6	75.7	66.0	70.0	60.5	46.5	73.3	71.1	45.7	28.5	26.4	63.1
Head2Toe-FT	43.9	82.3	53.5	84.9	76.7	86.5	24.5	79.9	95.9	77.5	74.3	68.0	70.9	48.2	72.4	76.1	44.8	32.1	42.5	65.0
Head2Toe-FT+	57.3	87.1	63.8	83.7	84.8	86.8	35.1	80.2	96.1	79.9	74.1	69.9	71.2	47.8	72.8	77.4	45.9	33.9	43.0	67.9

Table 1: Median test accuracy over 3 seeds on the VTAB-1k benchmark using pretrained (**top**) ResNet-50 and (**bottom**) ViT-B/16 backbones. Regularization baselines that use all layers are indicated with the +All prefix. "*" indicates results obtained from Zhai et al. (2019). Fine-tuning results for ViT-B/16 are obtained using the checkpoints provided by Dosovitskiy et al. (2021).

concatenated embedding. ViT-B/16 consists of 12 multi-headed self-attention layers. When we aggregate the output of the self-attention layers, we perform 1-D average pooling over the patch/token dimension choosing the pooling size to match a target number of features as before. Given that token dimension is permutation invariant, 1-D average pooling is unlikely to be the best choice here and a better aggregation function should provide further gains. We share a detailed list of intermediate representations utilized for each architecture in Appendix I and perform ablations on different alternatives in Appendix F.

HEAD2TOE selects a subset of features and trains a linear classifier without regularization on top of the selected features. We compare HEAD2TOE with regularization baselines that utilize all features. These baselines are denoted as +All- ℓ_1 , +All- ℓ_2 and +All- $\ell_{2,1}$ according to the regularizer norm they use.

We perform five-fold cross validation for each task and method in order to pick the best hyperparameters. All methods search over the same learning rates and training steps (two values of each). Methods that leverage intermediate features (i.e., regularization baselines and HEAD2TOE) additionally search over regularization coefficients and the *target size* of the aggregated representation at each layer. The FINETUNING baseline searches over 4 hyperparameters; thus the comparison of HEAD2TOE, which searches over 24 values, to fine-tuning might seem unfair. However, this was necessary due to fine-tuning being significantly more costly (about 200x on average) than training a linear classifier on intermediate features. We repeat each evaluation using 3 different seeds and report median values and share standard deviations in Appendix C. More details on hyperparameter selection and values used are shared in Appendix A.

4.1 RESNET-50

The top half of Table 1 presents results on the 19 VTAB-1k target domains when transferring from a pretrained ResNet-50 architecture. On average, HEAD2TOE slightly outperforms all other methods, including FINETUNING (see rightmost column of Table 1). HEAD2TOE, along with the regularization baselines that use intermediate layers, is far superior to LINEAR, indicating the value of the

intermediate layers. And HEAD2TOE is superior to the regularization baselines, indicating the value of explicit feature selection. Among the three categories of tasks, HEAD2TOE excels relative to the other methods for the *specialized* category, but does not outperform FINETUNING for the *natural* and *structured* categories.

Does HEAD2TOE select different features for each task? Which layers are used more frequently? In Appendix F, we show the distribution of features selected across different layers and the amount of intersection among features selected for different tasks and seeds. We observe high variation across tasks, motivating the importance of performing feature selection for each task separately. In addition to the fact that HEAD2TOE outperforms FINETUNING, it requires only 0.5% of FLOPs during training on average. Similarly, the cost of storing the adapted model is reduced to 1% on average. We discuss HEAD2TOE’s computational and storage costs in detail in Appendix B.

4.2 ViT-B/16

Results for ViT-B/16 are shared in the bottom half of Table 1. As with the ResNet-50 architecture, HEAD2TOE achieves the best accuracy among methods that keep the backbone fixed: HEAD2TOE improves accuracy over LINEAR by about 10% on average (in absolute performance), and HEAD2TOE outperforms the regularization baselines that include intermediate features but that do not explicitly select features. Similarly to the ResNet-50 experiments, HEAD2TOE matches the performance of FINETUNING. We share the distribution of features selected over layers in Appendix G.

Our goal in this work is to show that state-of-the-art performance can be obtained efficiently *without* changing the backbone itself. However, we expect to see further gains if the backbone is unfrozen and trained together with the final set of selected features. We perform some initial experiments to demonstrate the potential of such approach. After selecting features with HEAD2TOE, we fine-tune the backbone together with the final output layer (HEAD2TOE-FT) and observe around 2% increase in accuracy. We use the same light-weight validation procedure used for FINETUNING to pick the learning rate and training steps for the final fine-tuning steps. HEAD2TOE-FT provides significant gains over HEAD2TOE in the *structured* category, however performs poorly when transferring to some of the *natural* category tasks. Next, we determine whether or not to fine-tune the backbone by examining validation-set accuracy. This procedure, denoted HEAD2TOE-FT+, provides an additional 3% improvement and results in 67.9% accuracy over all VTAB-1k tasks, without any additional training or storage costs compared to FINETUNING.

4.3 UNDERSTANDING HEAD2TOE

HEAD2TOE selects individual features from a pre-trained backbone for each task separately and ignores the layer structure of the features. In this section we investigate different parts of the HEAD2TOE algorithm and compare them with some other alternatives. Additional experiments with fewer number of training examples and with different choice of candidate features can be found in Appendix F and Appendix G.

Relevance Scores. In Fig. 4-left, we demonstrate the effectiveness of group lasso on identifying relevant intermediate features of a ResNet-50 trained on ImageNet. We rank all features by their relevance score, s_i , and select groups of 2048 consecutive features beginning at a particular offset in this ranking. Offset 0 corresponds to selecting the features with largest relevance. We calculate average test accuracies across all VTAB tasks. As the figure shows, test accuracy decreases monotonically with the offset, indicating that the relevance score predicts the importance of including a feature in the linear classifier.

Selecting features or selecting layers? HEAD2TOE selects individual features independent of the layer in which they are embedded. We compare this *feature-wise* strategy to selecting layers as whole (i.e., selecting all features in a layer or none). One might expect *layer-wise* selection to be superior because it involves fewer decisions and therefore less opportunity to overfit to the validation set used for selecting the fraction F . Further, layer-wise selection may be superior because the relevance of one feature in a layer may indicate the relevance of others. To obtain a layer-wise relevance score, we compute the mean relevance score of all features in a layer and then rank layers by relevance.

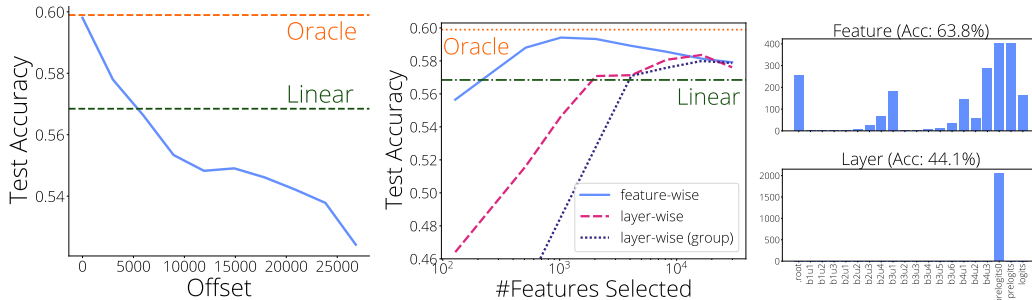


Figure 4: **(left)** Over all VTAB tasks, average accuracy of HEAD2TOE when selecting 2048 consecutive features sorted by their relevance score, starting with an index specified by *offset*. **(center)** Average accuracy over all VTAB tasks as a function of the number of features included. In this experiment, we only use features from the first layer of each of the 18 ResNet blocks and adjust pooling to have around 2048 features for each layer, totalling 29800 features. Results show that selecting layers performs worse than selecting features when adapting to a target domain. ORACLE results are explained in Section 3.3. **(right)** Distribution of 2048 intermediate features retained from a ResNet-50 when using feature-wise and layer-wise scores on the SVHN transfer task.

We also run an alternative layer selection algorithm, in which we group weights originating from the same layer together and select layers using the ℓ_2 norm of the groups, referred to as *layer-wise (group)*. Fig. 4-center compares feature-wise and layer-wise selection methods, matched for number of features retained. Feature-wise selection performs better than layer-wise selection on average and the best performance is obtained when around 1000 features are kept. We hypothesize that combining features across different layers provide better predictions, while including only the most important features from each layer reduces over-fitting. We share figures for the 19 individual tasks in Appendix E. Fig. 4-right shows the distribution of features selected from each layer by the feature-wise and layer-wise strategies for the SVHN transfer task.

Transfer across tasks. In practice, and in the literature, tasks are evaluated in isolation, i.e., the data from other tasks are not available. Nonetheless, in Fig. 5-left, we investigate how features selected using some task i performs when evaluated on a different task j . Each cell in the array represents the average accuracy over three seeds. For each column, we subtract the diagonal term (i.e., self-transfer, $i = j$) to obtain delta accuracy for each task. For most tasks, using a separate task for feature selection hurts performance. Results in Flowers-102 and Pets get better when other tasks like sNORB-Elev is used. Crucially no single task (rows of Fig. 5-left) yields features that are universally optimal, which highlights the importance of doing the feature selection during adaptation, not beforehand.

Similarity of features selected. In Fig. 5-right we investigate the intersection of features selected by HEAD2TOE. We select 2048 features for each task from the pool of 29800 features (same experiments as in Fig. 4-center). For each task HEAD2TOE selects a different subset of features. We calculate the fraction of features shared between each subset. For each target task we run 3 seeds resulting in 3 sets of features kept. When comparing the similarity across seeds (diagonal terms), we average over 6 possible combinations among these 3 sets. Similarly, when comparing two different datasets we average over 9 possible combinations. Both dSprites and sNORB images are generated artificially and have similar characteristics. Results show that such complementary tasks have the highest overlap, around 40%. Apart from a small fraction of datasets, however, most datasets seem to share less than 20% of the features, which highlights, again, the importance of doing the feature selection for each target task separately.

More candidate features for better results. HEAD2TOE often selects a few thousand features of the over one million features available. The high number of candidate features is critical for obtaining the best performance: in Fig. 6, we vary the number of intermediate features used for each of our pretrained backbones, indicated by line style. We observe that including all layers always performs better on average. However when varying the number of target features for each layer, we observed two distinct sub-groups of target tasks that behave differently as the number of features increases, indicated by the red and blue lines. This observation informed our decision to include

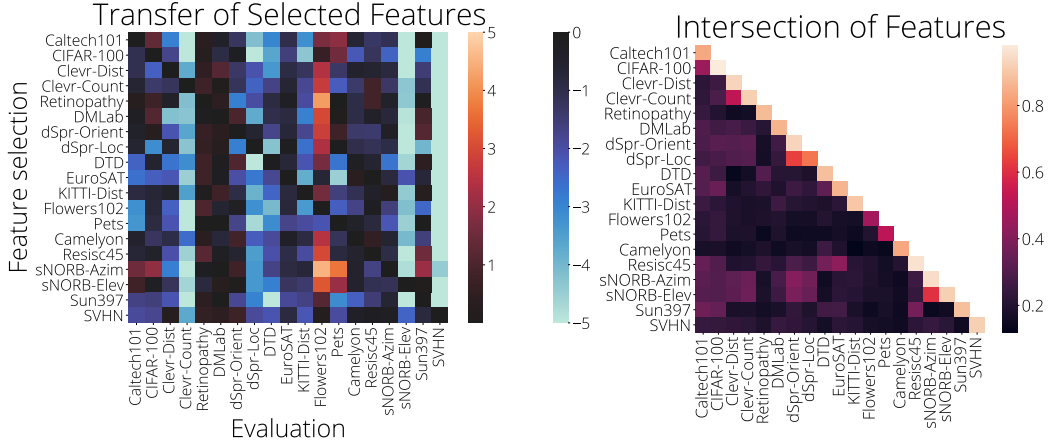


Figure 5: **(left)** Change in accuracy when features selected for a different task are used for adaptation. Most tasks get their best accuracy when the same task is also used for feature selection. **(right)** Intersection of features when selecting 2048 features from 29800 (same settings as in Fig. 4). The intersection is calculated as the fraction of features selected in two different runs. Values are averaged over 9 pairs of runs (3 seeds for each datasets), except the diagonal terms for which we remove identical pairs resulting in 6 pairs.

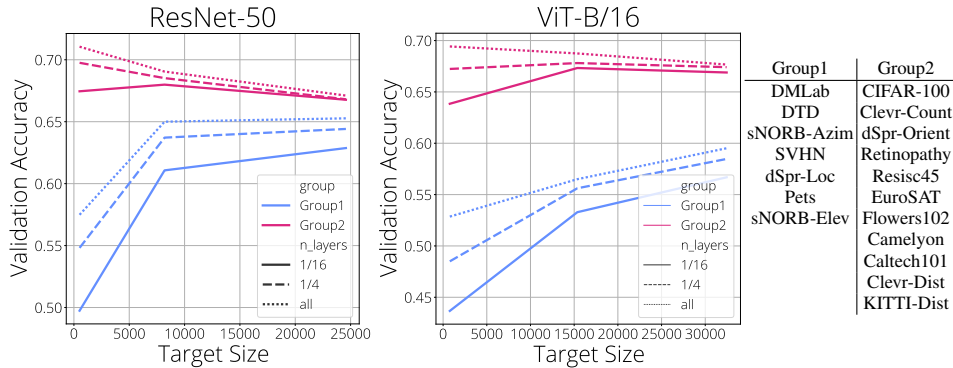


Figure 6: Effect of increasing the number of intermediate features that HEAD2TOE uses from the **(left)** ResNet-50 backbone and **(right)** ViT-B/16 backbone. The abscissa of the graph indicates the dimensionality of the representation extracted from each layer of the backbone (*target size*). The tasks are split into two groups (see right side of Figure), which show different behavior. The solid, dashed, and dotted lines indicate the fraction of layers selected for forming the representation used by HEAD2TOE: 1/16, 1/4, and 1, respectively. Scaling curves for individual tasks can be found in Appendix H.

both small and large target sizes in our validation hyperparameter search. Given the positive slope of the scaling curves, further increasing the number of available features for selection is a promising research direction.

5 RELATED WORK

Transfer Learning is studied extensively in the literature and used widely in practice. Most similar to our work is the work of Dalvi et al. (2019; 2020), which proposes a five-step method to select token representations from multiple locations in a pretrained model. They only consider the representation of the [CLS] token after the second MLP of the self-attention block, which makes the feature selection problem significantly smaller and as shown in Appendix G results in sub-optimal results. ELMo (Peters et al., 2018) averages two LSTM embeddings using a learned linear combination (a softmax) and requires embeddings to be same size. Thus, it is most similar to the suboptimal layer-selection baseline shown in Fig. 4-center. Given the ever increasing size and never saturating performance of pretrained models, the importance of reducing the cost of FINETUNING models is

stated in the literature regularly. Methods like feature-wise transformations (Bilen & Vedaldi, 2017), residual adapters (Houlsby et al., 2019; Rebuffi et al., 2017; Puigcerver et al., 2021), Diff-pruning (Guo et al., 2021) and selective fine-tuning (Guo et al., 2019; Fu et al., 2021) are proposed in order to reduce the cost of storing fine-tuned models. However, none of these methods match the simplicity of training (and storing) a linear classifier (i.e. HEAD2TOE) and they can be applied in conjunction with HEAD2TOE. Zhang et al. (2021) showed that selecting a sub-network of a pretrained model can increase OOD generalization. Teerapittayanon et al. (2016), Kaya et al. (2019), and Zhou et al. (2020) studied intermediate representations to reduce "overthinking" and thus provide better early-exit criteria. Similarly Baldock et al. (2021) showed a correlation between early classification of a sample and how easy its classification is. Intermediate features of a pretrained backbone are also used in object detection (Hariharan et al., 2015; Bell et al., 2016; Lin et al., 2017) and recently observed to improve the training of generative-adversarial networks Sauer et al. (2021).

Alternatives to transfer learning exist to learn from few labeled examples. Meta-learning (Thrun & Pratt, 1998; Schmidhuber, 1987; Schmidhuber et al., 1997) is used (among other things) to tackle the few-shot learning problem (i.e learning from limited data) from a learning-to-learn perspective; see Hospedales et al. (2020) for a comprehensive survey. In-between the representation learning and learning-to-learn paradigms lie approaches that use multi-domain training as an inductive bias, either without (Dvornik et al., 2020; Triantafillou et al., 2021; Li et al., 2021b;a) or with (Liu et al., 2021) meta-learning. However, in the large-scale setting FINE-TUNING remains a top-performing approach to few-shot classification (Dumoulin et al., 2021).

Feature selection aims to find the most relevant features from the input and is studied extensively in the machine-learning literature. Approaches can be grouped according to whether labeled data is used—supervised (Nie et al., 2010) or unsupervised (Ball & Hall, 1965; Hilborn & Lainiotis, 1967; He et al., 2005; Balin et al., 2019; Atashgahi et al., 2020)—or what high-level approach is taken—filter methods (Blum & Langley, 1997), wrapper methods (Kohavi & John, 1997), or embedded methods (Yuan & Lin, 2006). Most relevant to our work are embedded supervised methods as they have good scaling properties while achieving the best performance which is vital in our setting with over a million features. Embedded supervised feature selection methods use a cost function to iteratively refine the subset of features selected and popular approaches include forward selection (Viola & Jones, 2001; Borboudakis & Tsamardinos, 2019), backward selection (pruning) (Mozer & Smolensky, 1989; Guyon et al., 2004) and regularization/feature-ranking based methods (Yuan & Lin, 2006; Blum & Langley, 1997; Zhao et al., 2010). Most relevant to our work is Argyriou et al. (2007); Nie et al. (2010), both of which uses $\ell_{2,1}$ regularization to select features, however their approach requires matrix inversions which is not practical in our setting. We point interested readers to the survey of Gui et al. (2017) and book of Boln-Canedo et al. (2015) for a detailed discussion on the topic.

6 CONCLUSION

In this work, we introduced HEAD2TOE, an approach that extends linear probing (LINEAR) by selecting the most relevant features among a pretrained network’s intermediate representations. We motivated this approach in terms of a first-order Taylor series approximation to FINE-TUNING and show that the approach greatly improves performance over LINEAR and attains performance competitive with—and in some cases superior to—FINE-TUNING at much lower space and time complexity. Our findings challenge the conventional belief that FINE-TUNING is required to achieve good performance on OOD tasks. While more work is needed before HEAD2TOE can match the computational efficiency and simplicity of linear probing, our work paves the way for applying new and more efficient feature selection approaches and for experimenting with HEAD2TOE probing in other domains such as regression, video classification, object detection, reinforcement learning, and language modelling domains.

ACKNOWLEDGMENTS

We like to thank members of the Google Brain team for their useful feedback. Specifically we like to thank Cristina Vasconcelos, Eleni Triantafillou, Hossein Mobahi, Ross Goroshin for their feedback during the team meetings. We thank Joan Puigcerver, Fabian Pedregosa, Robert Gower, Laura Graesser, Rodolphe Jenatton for their feedback on the preprint. We thank Lucas Beyer and Xiaohua Zhai for creating the compact table for reporting VTAB results.

REFERENCES

- Zaid Alyafeai, Maged Saeed AlShaibani, and Irfan Ahmad. A survey on transfer learning in natural language processing. *arXiv preprint arXiv:2007.04239*, 2020.
- Andreas Argyriou, Theodoros Evgeniou, and Massimiliano Pontil. Multi-task feature learning. In B. Schölkopf, J. Platt, and T. Hoffman (eds.), *Advances in Neural Information Processing Systems*. MIT Press, 2007.
- Zahra Atashgahi, Ghada Sokar, Tim van der Lee, Elena Mocanu, Decebal Constantin Mocanu, Raymond N. J. Veldhuis, and Mykola Pechenizkiy. Quick and robust feature selection: the strength of energy-efficient sparse training for autoencoders. *ArXiv*, abs/2012.00560, 2020.
- R. Baldock, Hartmut Maennel, and Behnam Neyshabur. Deep learning through the lens of example difficulty. *ArXiv*, abs/2106.09647, 2021.
- Muhammed Fatih Balin, Abubakar Abid, and James Zou. Concrete autoencoders: Differentiable feature selection and reconstruction. In *Proceedings of the 36th International Conference on Machine Learning*, 2019.
- G. H. Ball and David J. Hall. Isodata, a novel method of data analysis and pattern classification. 1965.
- Charles Beattie, Joel Z Leibo, Denis Teplyashin, Tom Ward, Marcus Wainwright, Heinrich Küttler, Andrew Lefrancq, Simon Green, Víctor Valdés, Amir Sadik, et al. Deepmind lab. *arXiv preprint arXiv:1612.03801*, 2016.
- Sean Bell, C. Lawrence Zitnick, Kavita Bala, and Ross B. Girshick. Inside-outside net: Detecting objects in context with skip pooling and recurrent neural networks. *2016 IEEE Conference on Computer Vision and Pattern Recognition (CVPR)*, pp. 2874–2883, 2016.
- Hakan Bilen and Andrea Vedaldi. Universal representations: The missing link between faces, text, planktons, and cat breeds. *arXiv preprint arXiv:1701.07275*, 2017.
- Avrim L. Blum and Pat Langley. Selection of relevant features and examples in machine learning. *Artificial Intelligence*, 1997.
- Vernica Boln-Canedo, Noelia Snchez-Maroo, and Amparo Alonso-Betanzos. *Feature Selection for High-Dimensional Data*. Springer Publishing Company, Incorporated, 1st edition, 2015. ISBN 3319218573.
- Giorgos Borboudakis and I. Tsamardinos. Forward-backward selection with early dropping. *J. Mach. Learn. Res.*, 20:8:1–8:39, 2019.
- Gong Cheng, Junwei Han, and Xiaoqiang Lu. Remote sensing image scene classification: Benchmark and state of the art. *Proceedings of the IEEE*, 2017.
- M. Cimpoi, S. Maji, I. Kokkinos, S. Mohamed, , and A. Vedaldi. Describing textures in the wild. In *IEEE Conference on Computer Vision and Pattern Recognition*, 2014.
- Fahim Dalvi, Nadir Durrani, Hassan Sajjad, Yonatan Belinkov, Anthony Bau, and James R. Glass. What is one grain of sand in the desert? analyzing individual neurons in deep nlp models. In *AAAI*, 2019.
- Fahim Dalvi, Hassan Sajjad, Nadir Durrani, and Yonatan Belinkov. Analyzing redundancy in pre-trained transformer models. In *EMNLP*, 2020.
- Alexey Dosovitskiy, Lucas Beyer, Alexander Kolesnikov, Dirk Weissenborn, Xiaohua Zhai, Thomas Unterthiner, Mostafa Dehghani, Matthias Minderer, Georg Heigold, Sylvain Gelly, Jakob Uszkoreit, and Neil Houlsby. An image is worth 16x16 words: Transformers for image recognition at scale. In *International Conference on Learning Representations*, 2021. URL <https://openreview.net/forum?id=YicbFdNTTy>.

-
- Vincent Dumoulin, Neil Houlsby, Utku Evci, Xiaohua Zhai, Ross Goroshin, Sylvain Gelly, and Hugo Larochelle. Comparing transfer and meta learning approaches on a unified few-shot classification benchmark. *arXiv preprint arXiv:2104.02638*, 2021.
- Nikita Dvornik, Cordelia Schmid, and Julien Mairal. Selecting relevant features from a multi-domain representation for few-shot classification. In *European Conference on Computer Vision*, pp. 769–786. Springer, 2020.
- Cheng Fu, Hanxian Huang, Xinyun Chen, Yuandong Tian, and Jishen Zhao. Learn-to-share: A hardware-friendly transfer learning framework exploiting computation and parameter sharing. In *ICML*, 2021.
- Andreas Geiger, Philip Lenz, Christoph Stiller, and Raquel Urtasun. Vision meets robotics: The kitti dataset. *International Journal of Robotics Research*, 2013.
- Jie Gui, Zhenan Sun, Shuiwang Ji, Dacheng Tao, and Tieniu Tan. Feature selection based on structured sparsity: A comprehensive study. *IEEE Transactions on Neural Networks and Learning Systems*, 28:1490–1507, 2017.
- Demi Guo, Alexander M. Rush, and Yoon Kim. Parameter-efficient transfer learning with diff pruning. In *ACL/IJCNLP*, 2021.
- Yunhui Guo, Humphrey Shi, Abhishek Kumar, Kristen Grauman, Tajana Simunic, and Rogério Schmidt Feris. Spottune: Transfer learning through adaptive fine-tuning. *2019 IEEE/CVF Conference on Computer Vision and Pattern Recognition (CVPR)*, pp. 4800–4809, 2019.
- Isabelle Guyon, Jason Weston, Stephen D. Barnhill, and Vladimir Naumovich Vapnik. Gene selection for cancer classification using support vector machines. *Machine Learning*, 46:389–422, 2004.
- Bharath Hariharan, Pablo Arbeláez, Ross B. Girshick, and Jitendra Malik. Hypercolumns for object segmentation and fine-grained localization. *2015 IEEE Conference on Computer Vision and Pattern Recognition (CVPR)*, pp. 447–456, 2015.
- Xiaofei He, Deng Cai, and Partha Niyogi. Laplacian score for feature selection. In *Proceedings of the 18th International Conference on Neural Information Processing Systems*, 2005.
- Patrick Helber, Benjamin Bischke, Andreas Dengel, and Damian Borth. Eurosat: A novel dataset and deep learning benchmark for land use and land cover classification. *IEEE Journal of Selected Topics in Applied Earth Observations and Remote Sensing*, 2019.
- Charles G. Hilborn and Demetrios G. Lainiotis. The condensed nearest neighbor rule. 1967.
- Timothy Hospedales, Antreas Antoniou, Paul Micaelli, and Amos Storkey. Meta-learning in neural networks: A survey. *arXiv preprint arXiv:2004.05439*, 2020.
- Neil Houlsby, Andrei Giurgiu, Stanislaw Jastrzebski, Bruna Morrone, Quentin de Laroussilhe, Andrea Gesmundo, Mona Attariyan, and Sylvain Gelly. Parameter-efficient transfer learning for nlp. In *ICML*, 2019.
- Justin Johnson, Bharath Hariharan, Laurens van der Maaten, Li Fei-Fei, C Lawrence Zitnick, and Ross Girshick. Clevr: A diagnostic dataset for compositional language and elementary visual reasoning. In *IEEE Conference on Computer Vision and Pattern Recognition*, 2017.
- Kaggle and EyePacs. Kaggle diabetic retinopathy detection, July 2015. URL <https://www.kaggle.com/c/diabetic-retinopathy-detection/data>.
- Yigitcan Kaya, Sanghyun Hong, and T. Dumitras. Shallow-deep networks: Understanding and mitigating network overthinking. In *ICML*, 2019.
- Ron Kohavi and George H. John. Wrappers for feature subset selection. *Artif. Intell.*, 1997.

-
- Simon Kornblith, Jonathon Shlens, and Quoc V. Le. Do better imagenet models transfer better? *2019 IEEE/CVF Conference on Computer Vision and Pattern Recognition (CVPR)*, pp. 2656–2666, 2019.
- Alex Krizhevsky. Learning multiple layers of features from tiny images. Technical report, 2009.
- Yann LeCun, Fu Jie Huang, and Leon Bottou. Learning methods for generic object recognition with invariance to pose and lighting. In *IEEE Conference on Computer Vision and Pattern Recognition*, 2004.
- Fei-Fei Li, Rob Fergus, and Pietro Perona. One-shot learning of object categories. *IEEE Transactions on Pattern Analysis and Machine Intelligence*, 2006.
- Wei-Hong Li, Xialei Liu, and Hakan Bilen. Improving task adaptation for cross-domain few-shot learning. *arXiv preprint arXiv:2107.00358*, 2021a.
- Wei-Hong Li, Xialei Liu, and Hakan Bilen. Universal representation learning from multiple domains for few-shot classification. *arXiv preprint arXiv:2103.13841*, 2021b.
- Tsung-Yi Lin, Piotr Dollár, Ross B. Girshick, Kaiming He, Bharath Hariharan, and Serge J. Belongie. Feature pyramid networks for object detection. *2017 IEEE Conference on Computer Vision and Pattern Recognition (CVPR)*, pp. 936–944, 2017.
- Lu Liu, William Hamilton, Guodong Long, Jing Jiang, and Hugo Larochelle. A universal representation transformer layer for few-shot image classification. In *International Conference on Learning Representations*, 2021.
- Wesley Maddox, Shuai Tang, Pablo G. Moreno, Andrew Gordon Wilson, and Andreas C. Damianou. Fast adaptation with linearized neural networks. In *AISTATS*, 2021.
- Loic Matthey, Irina Higgins, Demis Hassabis, and Alexander Lerchner. dsprites: Disentanglement testing sprites dataset. <https://github.com/deepmind/dsprites-dataset/>, 2017.
- Michael C Mozer and Paul Smolensky. Skeletonization: A technique for trimming the fat from a network via relevance assessment. In *Advances in Neural Information Processing Systems*, 1989. URL <https://proceedings.neurips.cc/paper/1988/file/07e1cd7dca89a1678042477183b7ac3f-Paper.pdf>.
- Fangzhou Mu, Yingyu Liang, and Yin Li. Gradients as features for deep representation learning. *ArXiv*, abs/2004.05529, 2020.
- Basil Mustafa, Carlos Riquelme, Joan Puigcerver, and Andr’e Susano Pinto, Daniel Keysers, and Neil Houlsby. Deep ensembles for low-data transfer learning. *ArXiv*, abs/2010.06866, 2020.
- Yuval Netzer, Tao Wang, Adam Coates, Alessandro Bissacco, Bo Wu, and Andrew Y. Ng. Reading digits in natural images with unsupervised feature learning. In *NIPS Workshop on Deep Learning and Unsupervised Feature Learning 2011*, 2011.
- Feiping Nie, Heng Huang, Xiao Cai, and Chris Ding. Efficient and robust feature selection via joint $\ell_{2,1}$ -norms minimization. In J. Lafferty, C. Williams, J. Shawe-Taylor, R. Zemel, and A. Culotta (eds.), *Advances in Neural Information Processing Systems*, 2010.
- M-E. Nilsback and A. Zisserman. Automated flower classification over a large number of classes. In *Indian Conference on Computer Vision, Graphics and Image Processing*, Dec 2008.
- O. M. Parkhi, A. Vedaldi, A. Zisserman, and C. V. Jawahar. Cats and dogs. In *IEEE Conference on Computer Vision and Pattern Recognition*, 2012.
- Matthew E. Peters, Mark Neumann, Mohit Iyyer, Matt Gardner, Christopher Clark, Kenton Lee, and Luke Zettlemoyer. Deep contextualized word representations. In *NAACL*, 2018.
- Joan Puigcerver, Carlos Riquelme, Basil Mustafa, Cédric Renggli, André Susano Pinto, Sylvain Gelly, Daniel Keysers, and Neil Houlsby. Scalable transfer learning with expert models. *ArXiv*, abs/2009.13239, 2021.

-
- Sylvestre-Alvise Rebuffi, Hakan Bilen, and Andrea Vedaldi. Learning multiple visual domains with residual adapters. *arXiv preprint arXiv:1705.08045*, 2017.
- Olga Russakovsky, Jia Deng, Hao Su, Jonathan Krause, Sanjeev Satheesh, Sean Ma, Zhiheng Huang, Andrej Karpathy, Aditya Khosla, Michael Bernstein, Alexander C. Berg, and Li Fei-Fei. Imagenet large scale visual recognition challenge. *International Journal of Computer Vision (IJCV)*, 2015.
- Axel Sauer, Kashyap Chitta, Jens Müller, and Andreas Geiger. Projected gans converge faster. In *Advances in Neural Information Processing Systems (NeurIPS)*, 2021.
- Jürgen Schmidhuber. *Evolutionary principles in self-referential learning, or on learning how to learn: the meta-meta-... hook*. PhD thesis, Technische Universität München, 1987.
- Jürgen Schmidhuber, Jieyu Zhao, and Marco Wiering. Shifting inductive bias with success-story algorithm, adaptive levin search, and incremental self-improvement. *Machine Learning*, 28(1): 105–130, 1997.
- Surat Teerapittayanon, Bradley McDanel, and H. T. Kung. Branchynet: Fast inference via early exiting from deep neural networks. *2016 23rd International Conference on Pattern Recognition (ICPR)*, pp. 2464–2469, 2016.
- Sebastian Thrun and Lorien Pratt. Learning to learn: Introduction and overview. In *Learning to learn*, pp. 3–17. Springer, 1998.
- Eleni Triantafillou, Hugo Larochelle, Richard Zemel, and Vincent Dumoulin. Learning a universal template for few-shot dataset generalization. In *International Conference on Machine Learning*, 2021.
- Bastiaan S Veeling, Jasper Linmans, Jim Winkens, Taco Cohen, and Max Welling. Rotation equivariant cnns for digital pathology. In *International Conference on Medical Image Computing and Computer-Assisted Intervention*, 2018.
- Paul A. Viola and Michael J. Jones. Rapid object detection using a boosted cascade of simple features. *Proceedings of the 2001 IEEE Computer Society Conference on Computer Vision and Pattern Recognition. CVPR 2001*, 1:I–I, 2001.
- Songtao Wu, Shenghua Zhong, and Yan Liu. Deep residual learning for image steganalysis. *Multi-media Tools and Applications*, 2018.
- Jianxiong Xiao, James Hays, Krista A Ehinger, Aude Oliva, and Antonio Torralba. Sun database: Large-scale scene recognition from abbey to zoo. In *IEEE Conference on Computer Vision and Pattern Recognition*, 2010.
- Ming Yuan and Yi Lin. Model selection and estimation in regression with grouped variables. *Journal of The Royal Statistical Society Series B-statistical Methodology*, 68:49–67, 2006.
- Xiaohua Zhai, J. Puigcerver, Alexander Kolesnikov, P. Ruysen, Carlos Riquelme, Mario Lucic, Josip Djolonga, André Susano Pinto, Maxim Neumann, A. Dosovitskiy, L. Beyer, Olivier Bachem, M. Tschannen, Marcin Michalski, O. Bousquet, S. Gelly, and N. Houlsby. The visual task adaptation benchmark. *ArXiv*, abs/1910.04867, 2019.
- Dinghui Zhang, Kartik Ahuja, Yilun Xu, Yisen Wang, and Aaron C. Courville. Can subnetwork structure be the key to out-of-distribution generalization? In *ICML*, 2021.
- Zheng Zhao, L. Wang, and Huan Liu. Efficient spectral feature selection with minimum redundancy. In *AAAI*, 2010.
- Wangchunshu Zhou, Canwen Xu, Tao Ge, Julian McAuley, Ke Xu, and Furu Wei. Bert loses patience: Fast and robust inference with early exit. *ArXiv*, abs/2006.04152, 2020.
- Zhi-Hua Zhou, Jianxin Wu, and Wei Tang. Ensembling neural networks: Many could be better than all. *Artificial Intelligence*, 2002. URL <https://www.sciencedirect.com/science/article/pii/S000437020200190X>.

Zhuangdi Zhu, Kaixiang Lin, and Jiayu Zhou. Transfer learning in deep reinforcement learning: A survey. *arXiv preprint arXiv:2009.07888*, 2020.

Fuzhen Zhuang, Zhiyuan Qi, Keyu Duan, Dongbo Xi, Yongchun Zhu, Hengshu Zhu, Hui Xiong, and Qing He. A comprehensive survey on transfer learning. *Proceedings of the IEEE*, 109(1): 43–76, 2020.

AUTHOR CONTRIBUTIONS

- Utku: Proposed/planned/led the project, wrote the majority of the code, performed most experiments, wrote the initial draft of the paper.
- Vincent: Participated in weekly meetings for the project, reviewed code, contributed to framing the findings in terms of refuting the hypothesis that a pre-trained network lacks the features required to solve OOD classification tasks, helped with paper writing, helped run evaluations.
- Hugo: Helped identify and frame the research opportunity, attended regular meetings, contributed to analysis discussions, minor contributions to the writing.
- Mike: Participated in weekly meetings, confused matters due to his unfamiliarity with the literature, argued that the central idea of the paper was never going to work, contributed to framing research and helped substantially with the writing.

A HYPERPARAMETER SELECTION

We pick hyperparameters for each VTAB task separately by doing a 5-fold cross validation on the training data. For all methods, we chose the learning rate and the total number of training steps using the grid $lr = 0.1, 0.01$ and $steps = 500, 5000$, following the lightweight hyperparameter sweep recommended by the VTAB benchmark (Zhai et al., 2019).

For regularization baselines ℓ_1 , ℓ_2 and $\ell_{2,1}$ we search for regularization coefficients using (0.00001, 0.0001, 0.001). We include an extra value in this setting in order to account for the overhead introduced by HEAD2TOE.

For HEAD2TOE we choose $\ell_{2,1}$ regularization coefficients from (0.001, 0.00001) and target feature sizes from (1024, 16384, 40000) for ResNet-50 and (768, 15360, 32448) for ViT-B/16. After calculating feature scores HEAD2TOE validates the following fractions: (0.0005, 0.001, 0.002, 0.005, 0.01, 0.02, 0.05, 0.1) and thus requires 18% more operations compared to other regularization baselines. Note that this is because initial training to obtain feature scores s_i is performed once and therefore searching for optimal number of features has a small overhead. Hyper parameters selected by HEAD2TOE for each VTAB task are shared in Table 2 and Table 3. Next we explain how this overhead is estimated.

Dataset	Target Size	F	LR	Steps	$\ell_{2,1}$ Coef.
Caltech101	8192	0.010	0.01	5000	0.00001
CIFAR-100	512	0.200	0.01	500	0.00001
Clevr-Dist	8192	0.001	0.01	500	0.00100
Clevr-Count	512	0.005	0.10	5000	0.00100
Retinopathy	8192	0.200	0.01	500	0.00001
DMLab	8192	0.020	0.01	500	0.00001
dSpr-Orient	512	0.200	0.01	500	0.00001
dSpr-Loc	8192	0.005	0.10	500	0.00100
DTD	24576	0.005	0.01	5000	0.00001
EuroSAT	512	0.100	0.01	500	0.00001
KITTI-Dist	8192	0.020	0.01	500	0.00001
Flowers102	512	0.100	0.01	5000	0.00001
Pets	8192	0.002	0.01	5000	0.00001
Camelyon	512	0.020	0.10	500	0.00100
Resisc45	8192	0.020	0.01	500	0.00001
sNORB-Azim	24576	0.002	0.01	500	0.00001
sNORB-Elev	8192	0.050	0.01	500	0.00100
Sun397	512	0.100	0.01	5000	0.00100
SVHN	24576	0.005	0.01	500	0.00001

Table 2: Hyper parameters selected for the VTAB-1k benchmark tasks when using pretrained ResNet-50 backbone. F : fraction of features kept, LR: learning rate, Steps: Training Steps.

Dataset	Target Size	F	LR	Steps	$\ell_{2,1}$ Coef.
Caltech101	768	0.050	0.01	5000	0.00100
CIFAR-100	768	0.020	0.01	500	0.00001
Clevr-Dist	15360	0.002	0.01	500	0.00100
Clevr-Count	768	0.050	0.10	5000	0.00001
Retinopathy	768	0.010	0.01	500	0.00100
DMLab	32448	0.005	0.01	500	0.00001
dSpr-Orient	768	0.100	0.01	5000	0.00001
dSpr-Loc	32448	0.002	0.10	500	0.00100
DTD	768	0.100	0.01	500	0.00100
EuroSAT	768	0.100	0.01	500	0.00100
KITTI-Dist	32448	0.050	0.01	5000	0.00100
Flowers102	768	0.020	0.01	500	0.00001
Pets	768	0.020	0.01	5000	0.00100
Camelyon	768	0.100	0.01	500	0.00100
Resisc45	768	0.050	0.01	5000	0.00001
sNORB-Azim	32448	0.010	0.01	500	0.00001
sNORB-Elev	15360	0.200	0.01	500	0.00100
Sun397	768	0.050	0.01	5000	0.00100
SVHN	32448	0.005	0.01	500	0.00001

Table 3: Hyper parameters selected for the VTAB-1k benchmark tasks when using pretrained ViT-B/16 backbone. F : fraction of features kept, LR: learning rate, Steps: Training Steps.

Dataset	F	N	C	FLOPs (vs FINE TUNING)	Size (vs FINE TUNING)	Size (vs LINEAR)
Caltech101	0.010	467688	102	0.009675	0.020750	2.353167
CIFAR-100	0.200	30440	100	0.005792	0.025743	2.977301
Clevr-Dist	0.001	467688	6	0.005747	0.000741	1.417419
Clevr-Count	0.005	30440	8	0.000568	0.000092	0.132278
Retinopathy	0.200	467688	5	0.005657	0.020531	47.099634
DMLab	0.020	467688	6	0.005747	0.003011	5.756287
dSpr-Orient	0.200	30440	16	0.005302	0.004183	3.001686
dSpr-Loc	0.005	467688	16	0.006644	0.002212	1.587624
DTD	0.005	1696552	47	0.015823	0.019157	4.692396
EuroSAT	0.100	30440	10	0.005267	0.001336	1.532776
KITTI-Dist	0.020	467688	4	0.005567	0.002215	6.350983
Flowers102	0.100	30440	102	0.001117	0.013146	1.490882
Pets	0.002	467688	37	0.003842	0.002089	0.649417
Camelyon	0.020	30440	2	0.005220	0.000092	0.529114
Resisc45	0.020	467688	45	0.009247	0.018474	4.725480
sNORB-Azim	0.002	1696552	18	0.011069	0.004851	3.094923
sNORB-Elev	0.050	467688	9	0.006016	0.009578	12.210897
Sun397	0.100	30440	397	0.002839	0.049781	1.487498
SVHN	0.005	1696552	10	0.008464	0.005865	6.730334
Average				0.006295	0.010729	5.674742

Table 4: Relative cost of HEAD2TOE when compared with FINE TUNING and LINEAR. F is the fraction of features kept, N is the total number of features and C is the number of classes. On average HEAD2TOE requires 0.5% of the FLOPs required by FINE TUNING during the adaptation. Cost of storing each adapted model is also small: requiring only 1% of the FINE TUNING and only 5.7x more than LINEAR. See main text for details on how the numbers are calculated.

B COST OF HEAD2TOE

We evaluate different values of F and pick the value with best validation performance. Cost of HEAD2TOE consists of three parts: (1) C_I : Cost of calculating the representations using the pre-trained backbone. (2) C_{all} : cost of training the initial head \mathbf{W}_{all} (in order to obtain s_i 's) (3) $\sum_f C_{F=f}$: total cost of validating different values of F . Cost of validating a fraction value f , assuming equal number of training steps, is equal to $C_f = C_{all} * f$. Therefore relative cost of searching for F is equal to the sum of fractions validated (in comparison to the initial training of (s)).

In Table 4, we compare cost of running HEAD2TOE adaptation with FINETUNING. HEAD2TOE uses the backbone once in order to calculate the representations and then trains the \mathbf{W}_{all} , whereas FINETUNING requires a forward pass on the backbone at each step. Therefore we calculate the cost of fine-tuning for t steps as $C_I \cdot t$. Similarly, cost of HEAD2TOE is calculated as $C_I + C_{all} \cdot t$. The overall relative cost of C_{all} increases with number of classes C and number of features considered N . As shown in Table 1-top, HEAD2TOE obtains better results than FINETUNING, yet it requires 0.5% of the FLOPs needed on average.

After adaptation, all methods require roughly same number of FLOPs for inference due to all methods using the same backbone. The cost of storing models for each task becomes important when the same pre-trained backbone is used for many different tasks. In Table 4 we compare the cost of storing different models found by different methods. A fine-tuned model requires all weights to be stored which has the same cost as storing the original network, whereas LINEAR and HEAD2TOE requires storing only the output head: W_{linear} . HEAD2TOE also requires to store the indices of the features selected using a bitmap. Even though HEAD2TOE considers many more features during adaptation, it selects a small subset of the features and thus requires a much smaller final classifier (on average 1% of the FINETUNING). Note that hyper parameters are selected to maximize accuracy, not the size of the final model. We expect to see greater savings with an efficiency oriented hyperparameter selection.

C STANDARD DEVIATIONS FOR TABLE 1

In Table 5, we share the standard deviations for the median test accuracies presented in Table 1. On average we observe LINEAR obtains lower variation as expected, due to the limited adaptation and convex nature of the problem. Head2Toe seem to have similar (or less) variation then the other regularization baselines that use all features.

D ADDITIONAL PLOTS FOR EXPERIMENTS USING SINGLE ADDITIONAL LAYER

Test accuracies when using a single additional intermediate layer from a pretrained ResNet-50 backbone are shown in Fig. 7. *natural* datasets (except SVHN) are highly similar to upstream dataset (ImageNet-2012) and thus adding an extra intermediate layer doesn't improve performance much. However performance on OOD tasks (mostly of the tasks in *structured* category) improves significantly when intermediate representations are used, which correlates strongly with datasets in which HEAD2TOE exceeds FINETUNING performance.

E ADDITIONAL PLOTS FOR LAYER/FEATURE-WISE SELECTION COMPARISON

We compare layer-wise selection strategy discussed in Section 3 to HEAD2TOE in Fig. 8. For almost all datasets, feature-wise selection produces better results. Retinopathy and Flowers-102 are the only two datasets where the layer-wise strategy performs better.

	Natural							Specialized				Structured								Mean
	CIFAR-100	Caltech101	DTD	Flowers102	Pets	SVHN	Sun397	Camelyon	EuroSAT	Resisc45	Retinopathy	Clevr-Count	Clevr-Dist	DMLab	KITTI-Dist	dSpr-Loc	dSpr-Ori	sNORB-Azim	sNORB-Elev	
Linear	0.09	0.08	0.14	0.06	0.08	0.17	0.06	0.06	0.03	0.12	0.08	0.42	0.1	0.03	0.21	0.14	0.07	0.0	0.21	0.11
+All- ℓ_2	0.09	0.78	0.44	0.29	0.22	0.02	0.04	0.02	0.06	0.05	0.02	0.09	0.2	0.1	1.31	0.32	0.08	0.03	0.35	0.24
+All- ℓ_1	0.14	0.11	0.11	0.11	0.11	0.12	0.03	0.06	0.04	0.2	0.02	0.47	0.33	0.18	0.2	0.34	0.07	0.06	0.44	0.17
+All- $\ell_{2,1}$	0.09	1.0	0.13	0.1	0.1	0.18	0.23	0.15	0.07	0.09	0.05	0.03	0.08	0.11	0.41	0.51	0.24	0.16	0.07	0.2
Head2Toe	0.14	0.25	0.08	0.08	0.24	0.24	0.16	0.23	0.06	0.06	0.03	0.18	0.23	0.13	0.43	0.3	0.06	0.4	0.08	0.18

	Natural							Specialized				Structured								Mean
	CIFAR-100	Caltech101	DTD	Flowers102	Pets	SVHN	Sun397	Camelyon	EuroSAT	Resisc45	Retinopathy	Clevr-Count	Clevr-Dist	DMLab	KITTI-Dist	dSpr-Loc	dSpr-Ori	sNORB-Azim	sNORB-Elev	
Linear	0.1	0.23	0.19	0.16	0.06	0.06	0.08	0.09	0.08	0.06	0.0	0.06	0.02	0.07	0.92	0.21	0.08	0.08	0.03	0.14
+All- ℓ_2	0.13	0.17	0.0	0.66	0.36	0.04	0.56	0.02	0.59	0.01	0.04	0.23	0.13	0.12	1.24	0.28	0.09	0.84	0.2	0.3
+All- ℓ_1	0.06	0.11	0.15	0.08	0.19	0.31	0.08	0.08	0.06	0.12	0.05	0.28	0.17	0.23	0.87	0.34	0.07	0.22	0.28	0.2
+All- $\ell_{2,1}$	1.55	0.03	0.12	0.04	0.06	0.41	0.13	0.18	0.08	0.1	0.04	0.09	0.13	0.15	0.87	0.66	0.1	0.23	0.22	0.27
Head2Toe	0.29	0.16	0.26	0.5	0.19	0.14	0.07	0.13	0.04	0.09	0.09	0.04	0.44	0.14	1.34	0.21	0.01	0.31	0.08	0.24

Table 5: Standard deviation of test accuracy over 3 seeds on the VTAB-1k benchmark using pre-trained (**top**) ResNet-50 and (**bottom**) ViT-B/16 backbones. The mean column averages the standard deviations for each dataset.

F ADDITIONAL RESULTS FOR RESNET-50

Improvement of HEAD2TOE over fine-tuning test accuracy for ResNet-50 backbone is shown in Fig. 9. Similar to earlier plots, we observe a clear trend between being OOD and improvement in accuracy: HEAD2TOE obtains superior few-shot generalization for most of OOD tasks. We also share the distribution of features selected for each task in Fig. 10. Since different tasks might have different number features selected, we normalize each plot such that bars add up to 1. Overall, features from later layers seem to be preferred more often. Early layers are preferred, especially for OOD tasks like Clevr and sNORB. We observe a diverse set of distributions for selected features, which reflects the importance of selecting features from multiple layers. Even when distributions match, HEAD2TOE can select different features from the same layer for two different tasks. Therefore, next, we compare the indices of selected features directly to measure the diversity of features selected across tasks and seeds.

Effect of Training Data In Fig. 11, we compare the performance of HEAD2TOE with other baselines using reduced training data. Fraction (d_f)=1 indicates original tasks with 1000 training samples. For other fractions we calculate number of shots for each class as $\text{int}(1000 * f_d / C)$ where C is the number of classes and then sample a new version of the task accordingly. For SUN-397 task, number of shots are capped at 1 and thus fractions below 0.75 lead to 1-shot tasks and thus results are all the same. Overall we observe the performance of HEAD2TOE improves with amount of data available, possibly due to the reduced noise in feature selection.

Pre-activations or Activations? Taylor approximation of the fine-tuning presented in Section 3.1 suggests that the activations at every layer should be used. As an ablation we compare this approach with other alternatives in Table 6. Using only the CLS tokens at every layer without pooling (*Only CLS*) or appending the CLS token to the pooled representations (*Original+CLS*) didn't improve the results.

Including pooled input as a candidate for feature selection We also try providing (possibly pooled) input to HEAD2TOE. As shown in Table 2, this didn't improved the results and we got around 0.8% lower accuracy on average.

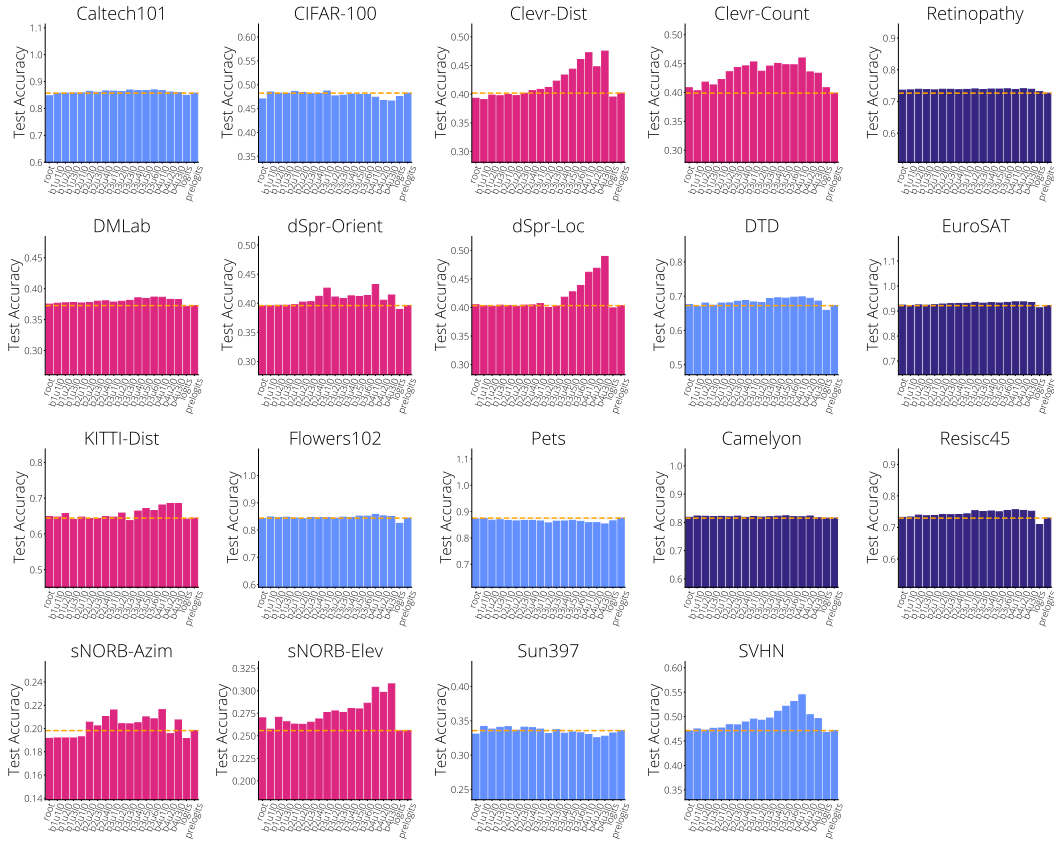


Figure 7: Test accuracies when using a single additional intermediate layer from a pretrained ResNet-50 backbone.

	Average	Natural	Specialized	Structured
Original	65.8	70.5	81.6	53.7
Pre-Normalization	63.5	67.4	81.1	51.3
Pre-Activation	63.5	67.4	81.3	51.3
Adding Pooled Input	65.0	69.7	81.2	52.9

Table 6: Ablation of choice of activations used on HEAD2TOE results for ResNet-50 backbone. Using features before the activation (*Pre-Activation*) or the normalization (*Pre-Normalization*) or adding the inputs to the pool of features considered bring worse results.

G ADDITIONAL RESULTS FOR VIT-B/16

Distribution of features across layers We share the distribution of features selected for each task in Fig. 12. As before, we normalize each plot such that bars add up to 1. Similar to ResNet-50, features from later layers selected more often for tasks from natural category. Early layers are preferred, especially for OOD tasks. In general distributions are more balanced, in other words, more intermediate features are used compared to ResNet-50.

Handling of CLS token Class (CLS) tokens in vision transformers are often added to the input and the classification layer is trained on top of the final representation of this token. Given that the representation of each token changes slowly, one might expect therefore the CLS representations along different layer to have more discriminate features. HEAD2TOE treats all tokens same and pools them together and in Table 7 we compare our approach with few other alternative approaches. Using only the CLS token at every layer without pooling (*Only CLS*) or appending the CLS token to the pooled representations (*Original+CLS*) doesn't improve the results.

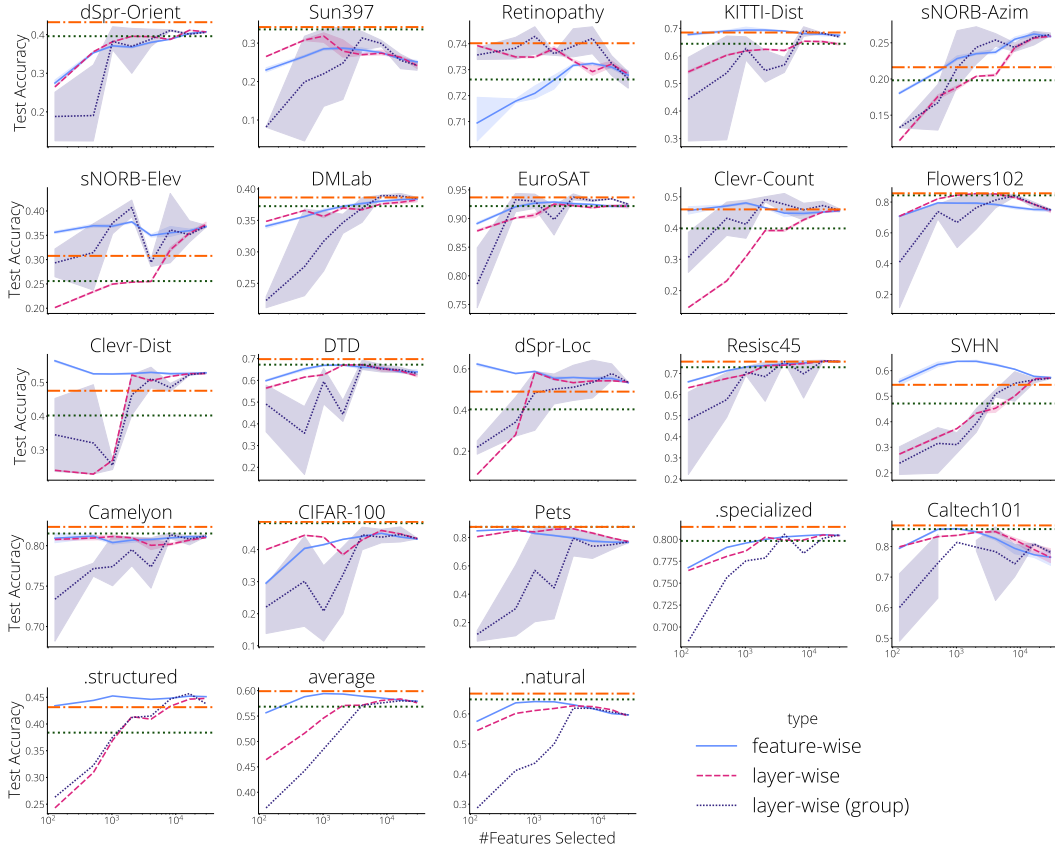


Figure 8: Test accuracies when varying the number of features selected for HEAD2TOE using a pretrained ResNet-50 backbone.

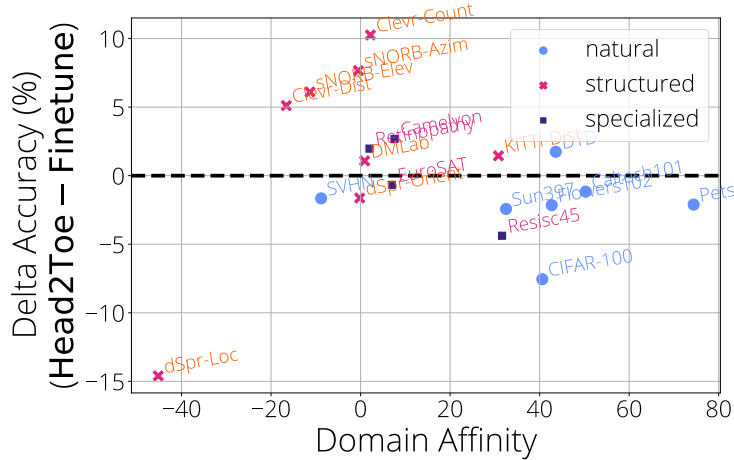


Figure 9: Accuracy improvement of HEAD2TOE compared to FINETUNING.

H ADDITIONAL PLOTS FOR SCALING BEHAVIOUR OF HEAD2TOE

Scaling behaviour of HEAD2TOE when using different feature target size and number of layers over 19 VTAB-1k tasks is shown in Fig. 13.



Figure 10: Distribution of selected features over different ResNet-50 layers for VTAB-1k tasks for results presented in Table 1. We group the layers in each block (group of 3 layers) to reduce numbers of bars.

	Average	Natural	Specialized	Structured
Original	63.3	71.3	82.6	46.7
Only CLS	57.3	65.1	81.4	38.4
Original+CLS	63.4	72.0	82.0	46.6

Table 7: Alternatives treatments for the CLS token of the ViT-B/16 architecture. Using only the CLS tokens at every layer without pooling (*Only CLS*) or appending the CLS token to the pooled representations (*Original+CLS*) doesn’t improve the results.

I DETAILS OF INTERMEDIATE REPRESENTATIONS INCLUDED

ResNet-50 has 5 stages. First stage includes a single convolutional layer (root) followed by pooling. We include features after pooling. Remaining stages include 3,4,6 and 3 bottleneck units (v2) each. Bottleneck units start with normalization and activation and has 3 convolutional layers. We includes features right after the activation function is applied, resulting in 3 intermediate feature sets per unit. Output after 5 stages are average-pooled and passed to the output head. We include features before and after pooling. with the output of the final layer (logits), total number of locations where features are extracted makes 52.

ViT-B/16 model consists of multiple encoder units. Each encoder unit consists of a self attention module followed by 2 MLPs. For each of these units, we include features (1) after layer-norm (but before self-attention) (2) features after self-attention (3-4) features after MLP layers (and after gelu

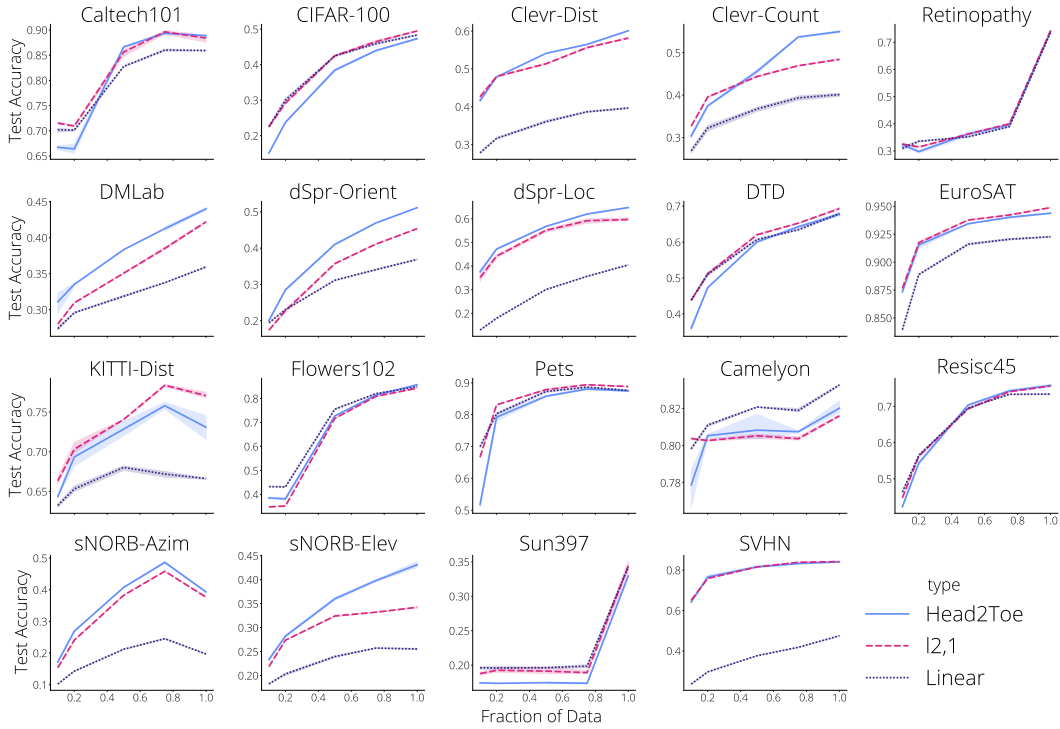


Figure 11: Effect of data available during training to the test accuracy. Fraction=1 indicates original tasks with 1000 training samples. Overall we observe the performance of HEAD2TOE improves with amount of data available, possibly due to the reduced noise in feature selection.

activation function). Additionally we use patched and embedded image (i.e. tokenized image input), pre-logits (final CLS-embedding) and logits.

J DETAILS OF DATASETS USED IN VTAB-1K BECHMARK

Table 8 include datasets used in VTAB-1k benchmark.



Figure 12: Distribution of selected features over different ViT-B/16 layers for VTAB-1k tasks for results presented in Table 1. We group the layers in encoder (group of 4 activations) to reduce numbers of bars.

Dataset	Classes	Reference
Caltech101	102	Li et al. (2006)
CIFAR-100	100	Krizhevsky (2009)
DTD	47	Cimpoi et al. (2014)
Flowers102	102	Nilsback & Zisserman (2008)
Pets	37	Parkhi et al. (2012)
Sun397	397	Xiao et al. (2010)
SVHN	10	Netzer et al. (2011)
EuroSAT	10	Helber et al. (2019)
Resisc45	45	Cheng et al. (2017)
Patch Camelyon	2	Veeling et al. (2018)
Retinopathy	5	Kaggle & EyePacs (2015)
Clevr/count	8	Johnson et al. (2017)
Clevr/distance	6	
dSprites/location	16	Matthey et al. (2017)
dSprites/orientation	16	
SmallNORB/azimuth	18	LeCun et al. (2004)
SmallNORB/elevation	9	
DMLab	6	Beattie et al. (2016)
KITTI/distance	4	Geiger et al. (2013)

Table 8: Datasets used in VTAB-1k benchmark.

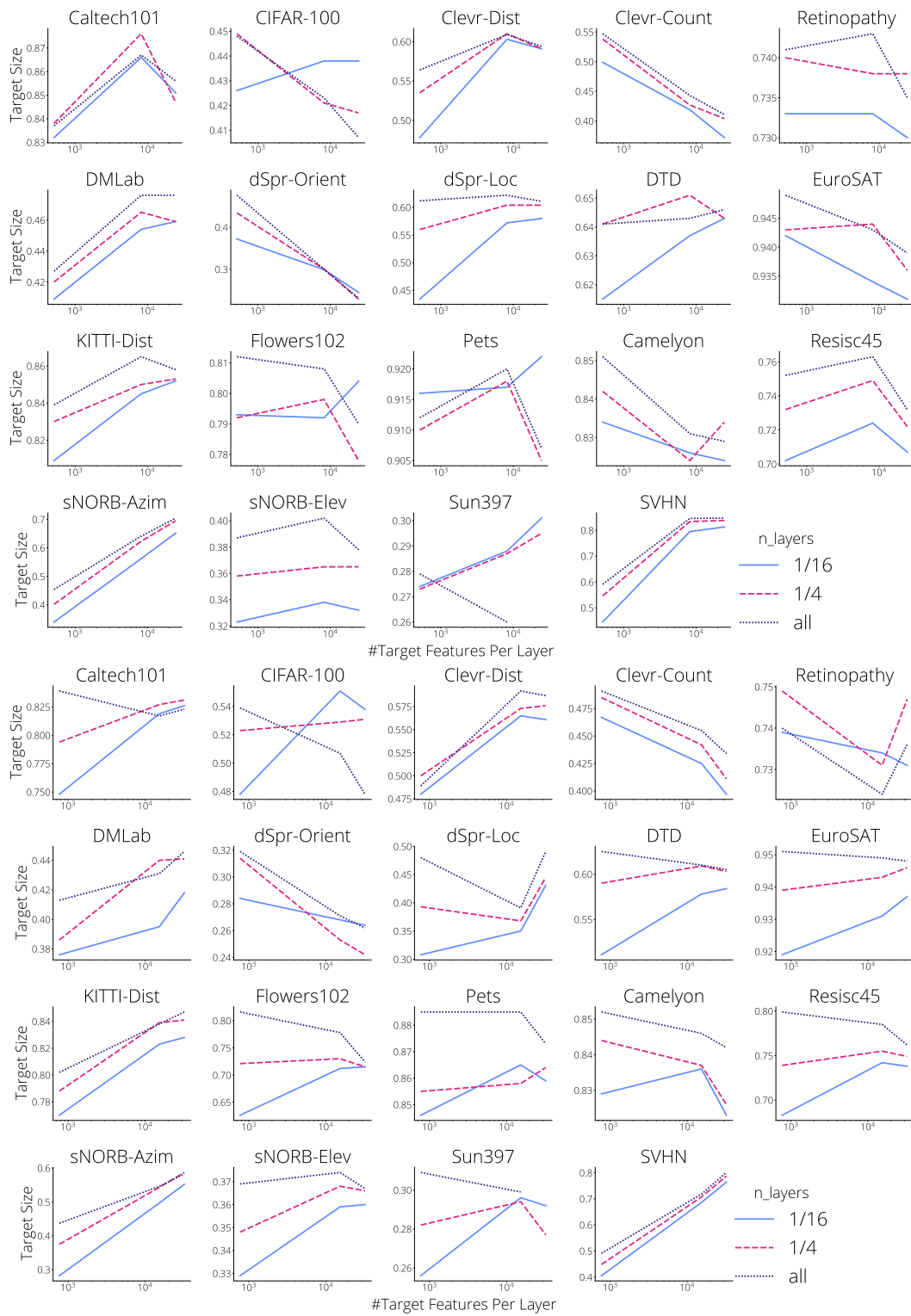


Figure 13: Scaling Behaviour over 19 VTAB-1k tasks when varying feature target size and number of layers utilized for **(top)** ResNet-50 and **(bottom)** ViT-B/16